Journal of Advanced Ceramics
2013, 2(2): 162–166
DOI: 10.1007/s40145-013-0056-y ISSN 2226-4108

Research Article

Preparation of rutile TiO_2 thin films by laser chemical vapor deposition method

Dongyun GUO[a,b,*], Akihiko ITO[b], Takashi GOTO[b], Rong TU[b], Chuanbin WANG[a], Qiang SHEN[a], Lianmeng ZHANG[a]

[a]*State Key Laboratory of Advanced Technology for Materials Synthesis and Processing, and School of Materials Science and Engineering, Wuhan University of Technology, Wuhan 430070, China*
[b]*Institute for Materials Research, Tohoku University, Sendai 980-8577, Japan*

Received: January 13, 2013; Revised: March 16, 2013; Accepted: March 18, 2013
©The Author(s) 2013. This article is published with open access at Springerlink.com

Abstract: TiO_2 thin films were prepared on Pt/Ti/SiO_2/Si substrate by laser chemical vapor deposition (LCVD) method. The effects of laser power (P_L) and total pressure (p_{tot}) on the microstructure of TiO_2 thin films were investigated. The deposition temperature (T_{dep}) was mainly affected by P_L, increasing with P_L increasing. The single-phase rutile TiO_2 thin films with different morphologies were obtained. The morphologies of TiO_2 thin films were classified into three typical types, including the powdery, Wulff-shaped and granular microstructures. p_{tot} and T_{dep} were the two critical factors that could be effectively used for controlling the morphology of the films.

Keywords: rutile TiO_2 thin film; laser chemical vapor deposition (LCVD); laser power; total pressure; microstructure

1 Introduction

The rutile TiO_2 films are widely investigated because they have many applications such as capacitors, sensors, antireflection coatings, and corrosion-resistant barriers [1–5]. The dielectric constant (ε_r) of the rutile TiO_2 crystal is anisotropic and has values of 170 in the *c* direction and 89 perpendicular to the *c* direction, which indicates that TiO_2 films have the possible application to future ultra-large-scale dynamic random access memory (DRAM) [6,7]. TiO_2 films have been prepared by many methods, including sputtering, conventional chemical vapor deposition, sol–gel method, type-casting, and laser chemical vapor deposition (LCVD) [8–15]. Among these methods, LCVD is considered to be a promising process to prepare high-quality films with controllability of microstructure and orientation at high deposition rate (R_{dep}) [16–21]. In LCVD process, the morphology and orientation of the films are affected by various parameters, such as laser power (P_L), total pressure (p_{tot}) in LCVD chamber, pre-heating temperature (T_{pre}), and precursor evaporation temperature. In our previous study, the rutile TiO_2 thick films with random orientation were prepared by LCVD with ε_r = 73, and the morphology and orientation of TiO_2 thick films were controlled by the variation of P_L [20,21].

In the present study, TiO_2 thin films are prepared on Pt/Ti/SiO_2/Si substrate by LCVD, and the effects of p_{tot} and P_L on the orientation and microstructure of TiO_2 thin films are investigated.

* Corresponding author.
E-mail: guodongyun@gmail.com

2 Experiment

TiO_2 thin films were prepared on $Pt/Ti/SiO_2/Si$ substrate by LCVD with a continuous-wave Nd:YAG laser (wavelength = 1064 nm). A schematic of LCVD apparatus has been reported elsewhere [16,19]. The substrate was heated on a hot stage at T_{pre} = 773 K. A thermocouple was inserted at the bottom side of the substrate to measure the deposition temperature (T_{dep}). A laser beam expanded to about 16 mm in diameter was introduced through a quartz window to irradiate the whole $Pt/Ti/SiO_2/Si$ substrate. P_L was changed from 48 W to 98 W. The titanium diisopropoxy-dipivaloylmethanate ($Ti(Oi\text{-}Pr)_2(DPM)_2$, Toshima Manufactory) precursor was heated at 423 K, and the vapor was carried into the chamber with Ar gas. O_2 gas was separately introduced into the chamber through a double-tube gas nozzle. p_{tot} in LCVD chamber was varied from 400 Pa to 950 Pa. The deposition was conducted for 300 s. Details of the deposition conditions are listed in Table 1.

Table 1 Deposition conditions of TiO_2 thin films prepared by LCVD

$Ti(Oi\text{-}Pr)_2(DPM)_2$ evaporation temperature (T_{Ti})	423 K
Substrate pre-heating temperature (T_{pre})	773 K
Total chamber pressure (p_{tot})	400–950 Pa
Gas flow rate	
Ar gas (FR_{Ar})	8.3×10^{-7} m^3/s
O_2 gas (FR_{O_2})	1.7×10^{-6} m^3/s
Laser power (P_L)	48–98 W
Deposition time (t)	300 s
Substrate–nozzle distance	30 mm
Substrate	$Pt/Ti/SiO_2/Si$ (10 mm × 10 mm × 0.5 mm)

The crystal structure of TiO_2 thin films was analyzed by X-ray diffraction (XRD, Rigaku RAD-2C) using Cu Kα radiation. The surface and cross-sectional microstructures of TiO_2 thin films were observed by a field-effect scanning electron microscope (FE-SEM, JSM 6335F).

3 Results and discussion

Figure 1 shows the relationship between p_{tot} and T_{dep} of TiO_2 thin films prepared at different P_L. At the same p_{tot}, with increasing P_L, T_{dep} also increases. As P_L is fixed, T_{dep} slightly changes with increasing p_{tot}, which indicates that the relationship between T_{dep} and p_{tot} is very small. These results indicate that T_{dep} is mainly affected by P_L.

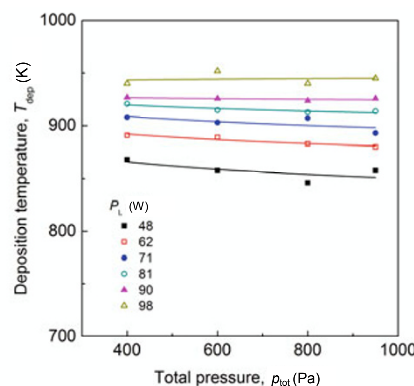

Fig. 1 Relationship between T_{dep} and p_{tot} of TiO_2 thin films prepared at different P_L.

Figure 2 depicts the typical XRD patterns of TiO_2 thin films prepared at P_L = 98 W with different p_{tot}. The XRD patterns are indexed to the rutile TiO_2 phase (JCPDS 21-1276). The single-phase TiO_2 thin films are obtained, and the intensity of (110) peak decreases with increasing p_{tot}, which indicates that the crystallinity of the films becomes worse. In our previous study, the orientation of TiO_2 films changed from random to (110) orientation with increasing P_L from 48 W to 98 W at $Ti(Oi\text{-}Pr)_2(DPM)_2$ evaporation temperature T_{Ti} = 433 K [21]. However, in this study, all TiO_2 thin films prepared at different p_{tot} and P_L show the (110) orientation at T_{Ti} = 423 K. T_{Ti} affects the pressure of Ti vapor, which further influences the gas-phase supersaturation. The supersaturation is one of the important parameters to control the structure of TiO_2 films [22].

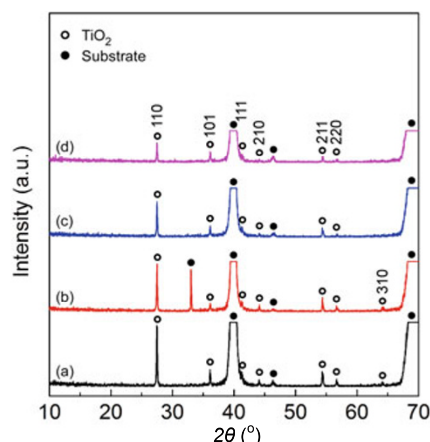

Fig. 2 XRD patterns of TiO_2 thin films prepared at P_L = 98 W and different p_{tot}: (a) 400 Pa, (b) 600 Pa, (c) 800 Pa and (d) 950 Pa.

The surface and cross-sectional SEM images of TiO_2 thin films are shown in Fig. 3. In this study, the morphologies of all TiO_2 thin films are classified into three types. When TiO_2 thin film is prepared at p_{tot} = 400 Pa and P_L = 90 W (T_{dep} = 927 K), the film shows the powdery microstructure, as shown in Figs. 3(a) and 3(b). Kimura [23] reported that the powder was formed in gas phase due to the high T_{dep} when he prepared yttria-stabilized zirconia films by LCVD method. TiO_2 thin film prepared at p_{tot} = 800 Pa and P_L = 98 W (T_{dep} = 940 K) mainly consists of the Wulff-shaped grains with the columnar cross-section (Figs. 3(c) and 3(d)). Wulff construction gives the equilibrium crystal shape of a macroscopic crystal, and the Wulff-shaped rutile grains are commonly observed when the rutile nanocrystals are prepared [1,24]. The film prepared at p_{tot} = 950 Pa and P_L = 48 W (T_{dep} = 858 K) shows the granular microstructure and columnar cross-section, as shown in Figs. 3(e) and 3(f). Figure 4 displays the effects of p_{tot} and T_{dep} on the morphology of TiO_2 thin films. For TiO_2 thin films prepared at p_{tot} = 400 Pa and T_{dep} = 921–940 K (P_L = 81–98 W), and p_{tot} = 600 Pa and T_{dep} = 952 K (P_L = 98 W), they have the typical powdery microstructure. The powdery microstructure increases the surface area, which could result in superior photochemical properties of TiO_2 thin films. For TiO_2 thin films prepared at p_{tot} = 400 Pa and T_{dep} = 891–908 K (P_L = 62–71 W), p_{tot} = 600 Pa and T_{dep} = 903–926 K (P_L = 71–90 W), p_{tot} = 800 Pa and T_{dep} = 924–940 K (P_L = 90–98 W), and p_{tot} = 950 Pa and T_{dep} = 926–945 K (P_L = 90–98 W), they consist of the typical Wulff-shaped grains. When TiO_2 thin films are prepared at p_{tot} = 400 Pa and T_{dep} = 868 K (P_L = 48 W), p_{tot} = 600 Pa and T_{dep} = 858–889 K (P_L = 48–62 W), p_{tot} = 800 Pa and T_{dep} = 846–913 K (P_L = 48–81 W), and p_{tot} = 950 Pa and T_{dep} = 858–914 K (P_L = 48–81 W), they show the typical granular microstructure.

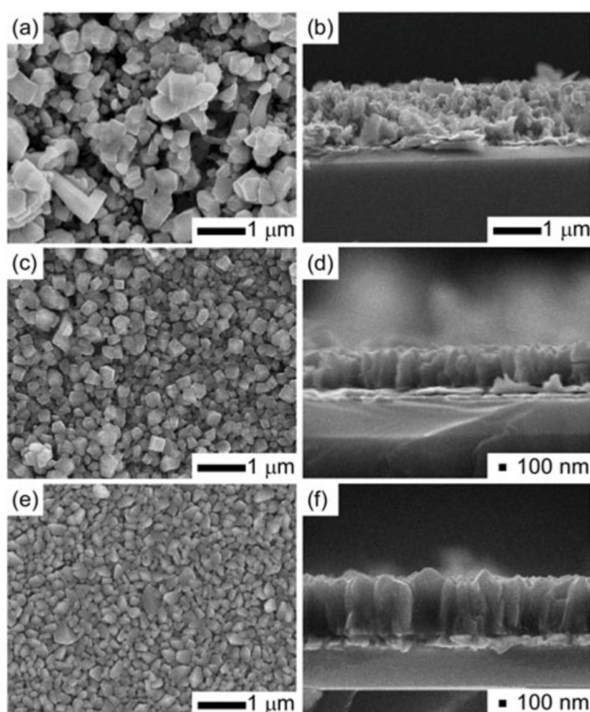

Fig. 3 Typical surface and cross-sectional images of TiO_2 thin films prepared at different p_{tot} and P_L: (a) and (b) 400 Pa and 90 W (T_{dep} = 927 K); (c) and (d) 800 Pa and 98 W (T_{dep} = 940 K); (e) and (f) 950 Pa and 48 W (T_{dep} = 858 K).

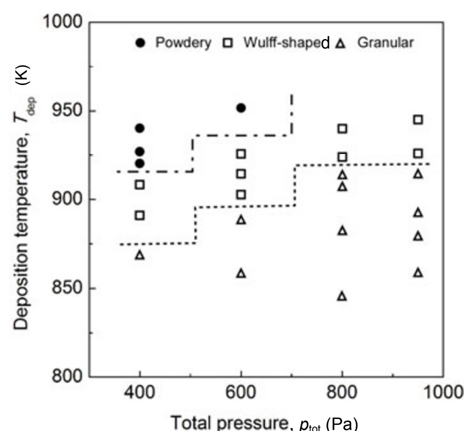

Fig. 4 Effects of p_{tot} and T_{dep} on the morphology of TiO_2 thin films.

Figure 5 demonstrates the relationship between R_{dep} and T_{dep} of TiO_2 thin films prepared at different p_{tot} in Arrhenius format. R_{dep} is obtained according to the cross-sectional SEM images of all TiO_2 thin films. R_{dep} slightly changes with the variation of T_{dep}, while R_{dep} obviously decreases with p_{tot} increasing.

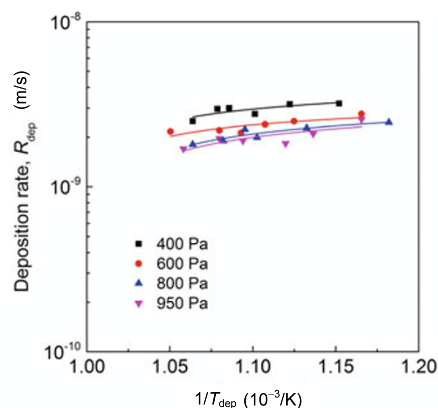

Fig. 5 Relationship between R_{dep} and T_{dep} of TiO_2 thin films prepared at different p_{tot} in Arrhenius format.

4 Conclusions

The single-phase rutile TiO_2 thin films were prepared on $Pt/Ti/SiO_2/Si$ substrate by LCVD. When the films were prepared at the same p_{tot}, T_{dep} increased with increasing P_L. As P_L was fixed, T_{dep} slightly decreased with increasing p_{tot}. The morphologies of TiO_2 thin films were classified into three typical types, including the powdery, Wulff-shaped and granular microstructures. p_{tot} and T_{dep} were the two critical factors that could be effectively used for controlling the morphology of the films. R_{dep} slightly changed with the variation of T_{dep}, while R_{dep} obviously decreased with p_{tot} increasing.

Acknowledgements

This work was supported in part by the Global COE Program of the Materials Integration, Tohoku University, and the International Science and Technology Cooperation Program of China (Grant No. 2009DFB50470). This work was also supported in part by the International Science and Technology Cooperation Project of Hubei Province (Grant No. 2010BFA017) and the 111 Project of China (Grant No. B13035).

Open Access: This article is distributed under the terms of the Creative Commons Attribution Noncommercial License which permits any noncommercial use, distribution, and reproduction in any medium, provided the original author(s) and source are credited.

References

[1] Diebold U. The surface science of titanium dioxide. *Surf Sci Rep* 2003, **48**: 53–229.

[2] Kadoshima M, Hiratani M, Shimamoto Y, *et al*. Rutile-type TiO_2 thin film for high-*k* gate insulator. *Thin Solid Films* 2003, **424**: 224–228.

[3] Hanaor DAH, Sorrell CC. Review of the anatase to rutile phase transformation. *J Mater Sci* 2011, **46**: 855–874.

[4] Fujishima A, Zhang XT, Tryk DA. TiO_2 photocatalysis and related surface phenomena. *Surf Sci Rep* 2008, **63**: 515–582.

[5] Fujishima A, Honda K. Electrochemical photolysis of water at a semiconductor electrode. *Nature* 1972, **238**: 37–38.

[6] Parker RA. Static dielectric constant of rutile (TiO_2), 1.6–1060°K. *Phys Rev* 1961, **124**: 1719–1722.

[7] Kim SK, Kim W-D, Kim K-M, *et al*. High dielectric constant TiO_2 thin films on a Ru electrode grown at 250 ℃ by atomic-layer deposition. *Appl Phys Lett* 2004, **85**: 4112.

[8] Alexandrov P, Koprinarova J, Todorov D. Dielectric properties of TiO_2-films reactively sputtered from Ti in an RF magnetron. *Vacuum* 1996, **47**: 1333–1336.

[9] Rausch N, Burte EP. Thin TiO_2 films prepared by low pressure chemical vapor deposition. *J Electrochem Soc* 1993, **140**: 145–149.

[10] Zhang QM, Griffin GL. Gas-phase kinetics for TiO_2 CVD: Hot-wall reactor results. *Thin Solid Films* 1995, **263**: 65–71.

[11] Kim JY, Jung HS, No JH, *et al*. Influence of anatase–rutile phase transformation on dielectric properties of sol–gel derived TiO_2 thin films. *J Electroceram* 2006, **16**: 447–451.

[12] Oja I, Mere A, Krunks M, *et al*. Structural and electrical characterization of TiO_2 films grown by spray pyrolysis. *Thin Solid Films* 2006, **515**: 674–677.

[13] Chao S, Dogan F. Processing and dielectric properties of TiO_2 thick films for high-energy density capacitor applications. *Int J Appl Ceram Tec* 2011, **8**: 1363–1373.

[14] Gao M, Ito A, Tu R, *et al*. Microcolumnar and granular structures of TiO_2 films prepared by laser CVD using Nd:YAG laser. *Key Eng Mat* 2012, **508**: 287–290.

[15] Goto T, Kimura T. Laser chemical vapor deposition of thick oxide coatings. *Key Eng Mat* 2006, **317–318**: 495–500.

[16] Guo DY, Goto T, Wang CB, *et al*. High-speed growth of (103)-oriented Ba_2TiO_4 film by laser chemical vapor deposition. *Mater Lett* 2012, **70**: 135–137.

[17] Guo DY, Ito A, Tu R, *et al*. High-speed epitaxial growth of $BaTi_2O_5$ films and their in-plane orientations. *Appl Surf Sci* 2012, **259**: 178–185.

[18] Guo DY, Ito A, Goto T, *et al*. Dielectric properties of $Ba_4Ti_{13}O_{30}$ film prepared by laser chemical vapor deposition. *J Mater Sci* 2012, **47**: 1559–1561.

[19] Guo DY, Goto T, Wang CB, *et al*. High-speed preparation and dielectric properties of $BaTi_4O_9$ film by laser chemical vapor deposition. *J Mater Sci: Mater El* 2012, **23**: 897–900.

[20] Guo DY, Ito A, Goto T, *et al*. Preparation of TiO_2 thick film by laser chemical vapor deposition method. *J Mater Sci: Mater El* 2012, DOI: 10.1007/s10854-012-1008-y.

[21] Guo DY, Ito A, Goto T, *et al*. Effect of laser power

on orientation and microstructure of TiO_2 films prepared by laser chemical vapor deposition method. *Mater Lett* 2013, **93**: 179–182.

[22] Zeng JH, Yu YL, Wang YF, *et al*. High-density arrays of low-defect-concentration zinc oxide nanowire grown on transparent conducting oxide glass substrate by chemical vapor deposition. *Acta Mater* 2009, **57**: 1813–1820.

[23] Kimura T. High-speed deposition of yttria-stabilized zirconia and titania films by laser chemical vapor deposition. *J Ceram Soc Jpn* 2006, **114**: 161–166.

[24] Hong ZS, Wei MD, Lan TB, *et al*. Self-assembled nanoporous rutile TiO_2 mesocrystals with tunable morphologies for high rate lithium-ion batteries. *Nano Energy* 2012, **1**: 466–471.